Kesebolite-(Ce), CeCa$_2$Mn(AsO$_4$)[SiO$_3$]$_3$, a New REE-Bearing Arsenosilicate Mineral from the Kesebol Mine, Åmål, Västra Götaland, Sweden

Dan Holtstam [1,*] , **Luca Bindi** [2] , **Andreas Karlsson** [1] , **Jörgen Langhof** [1], **Thomas Zack** [3,4], **Paola Bonazzi** [2] **and Anders Persson** [5]

1   Department of Geosciences, Swedish Museum of Natural History, P.O. Box 50007,
    SE-104 05 Stockholm, Sweden; andreas.karlsson@nrm.se (A.K.); jorgen.langhof@nrm.se (J.L.)
2   Dipartimento di Scienze della Terra, Università degli Studi di Firenze, Via G. La Pira 4, I-50121 Firenze, Italy;
    luca.bindi@unifi.it (L.B.); paola.bonazzi@unifi.it (P.B.)
3   Department of Earth Sciences, University of Gothenburg, P.O. Box 460, SE-405 30 Göteborg, Sweden;
    thomas.zack@gu.se
4   Department of Earth Sciences, University of Adelaide, Adelaide, SA 5005, Australia
5   Parkgatan 14, SE-671 32 Arvika, Sweden; kpanderspersson@telia.com
*   Correspondence: dan.holtstam@nrm.se; Tel.: +46-8-5195-4234

Abstract: Kesebolite-(Ce), ideal formula CeCa$_2$Mn(AsO$_4$)[SiO$_3$]$_3$, is a new mineral (IMA No. 2019-097) recovered from mine dumps at the Kesebol Mn-(Fe-Cu) deposit in Västra Götaland, Sweden. It occurs with rhodonite, baryte, quartz, calcite, talc, andradite, rhodochrosite, K-feldspar, hematite, gasparite-(Ce), chernovite-(Y) and ferriakasakaite-(Ce). It forms mostly euhedral crystals, with lengthwise striation. The mineral is dark grayish-brown to brown, translucent, with light brown streak. It is optically biaxial (+), with weak pleochroism, and n_{calc} = 1.74. H = 5–6 and VHN$_{100}$ = 825. Fair cleavage is observed on {100}. The calculated density is 3.998(5) g·cm^{-3}. Kesebolite-(Ce) is monoclinic, $P2_1/c$, with unit-cell parameters from X-ray single-crystal diffraction data: a = 6.7382(3), b = 13.0368(6), c = 12.0958(6) Å, β = 98.578(2)°, and V = 1050.66(9) Å^3, with Z = 4. Strongest Bragg peaks in the X-ray powder pattern are: [I(%), d(Å) (hkl)] 100, 3.114 (20-2); 92, 2.924 (140); 84, 3.138 (041); 72, 2.908 (014); 57, 3.228 (210); 48, 2.856 (042); 48, 3.002 (132). The unique crystal structure was solved and refined to $R1$ = 4.6%. It consists of 6-periodic single silicate chains along (001); these are interconnected to infinite (010) strings of alternating, corner-sharing MnO$_6$ and AsO$_4$ polyhedra, altogether forming a trellis-like framework parallel to (100).

Keywords: kesebolite-(Ce); new mineral; crystal structure; arsenosilicate; rare earth elements; cerium anomaly; skarn; Sweden

1. Introduction

Manganese-arsenosilicates form rare kinds of minerals with ca. 20 species known to date. Most of them are typical products of late-stage mineralization in hydrothermally reworked Mn deposits. Here we present the description of the first nominally Ca and REE-bearing mineral belonging to this category, kesebolite-(Ce), ideally CeCa$_2$Mn(AsO$_4$)[SiO$_3$]$_3$. The new mineral species and its name were approved by the Commission on New Minerals, Nomenclature and Classification, International Mineralogical Association (No. 2019-097). The name is for the discovery locality, the Kesebol mine, in the Åmål municipality, Västra Götaland, Sweden (lat. 58°59.06′ N, long. 12°31.79′ E, elevation 130 m a.s.l.). Kesebol, pronounced [ɕe:sebu:l] with a "soft" Swedish k, is also the name of a nearby farm. The name

"kesebolit" had previously been used for a variety of jacobsite, $MnFe_2O_4$; it occurs in an unpublished report [1] and is thus not entrenched in the scientific literature.

The holotype specimen of kesebolite-(Ce) is preserved in the type mineral collection of the Department of Geosciences, Swedish Museum of Natural History, Box 50007, SE-10405 Stockholm, Sweden, under collection no. GEO-NRM 20100343.

2. Occurrence

The Kesebol Mn-(Fe-Cu) deposit belongs to a group of mostly sub-economic Mn occurrences along the SW shore of Lake Vänern, Sweden and the EU's largest lake. More than 40,000 metric tonnes of Mn ore were, however, produced in the period 1917–1944 from a single deposit, the Kesebol mine, along with lesser amounts of Cu [2]. Mining efforts occurred down to 110 m depth [3]. Felsic metavolcanic rocks of the Åmål formation, comprising 1.63–1.59 Ga supracrustal units of the Fennoscandian Shield [4] host the ores. Deformational, metamorphic and metallogenic processes have affected the region during the Sveconorwegian (1.1–0.9 Ga, commonly grouped with the Grenville) orogeny [5,6]. Lead isotope data obtained from sulfide mineralization in the Kesebol deposit indicate a link to this orogenic event [7].

The Kesebol ores are breccia- and fracture-filling mineralizations bound to a narrow line along a N–S brittle-deformation zone in a fine-grained rhyolitic rock with quartz phenocrysts [2]. The Mn ores consist of two essentially spatially separated units: fine-grained oxide mineralization (hausmannite ± jacobsite) and carbonate-silicate mineralization (rhodochrosite + manganoan calcite + rhodonite + manganoan garnet). Late-stage alteration formed Mn^{4+}-bearing oxides and hydrous Mn-silicates that occur in veins. A few rare Ce- and As-bearing minerals have been identified in recent times, from assemblages associated with Mn ore: gasparite-(Ce), chernovite-(Y), ferriakasakaite-(Ce), retzian-(Ce), sarkinite and flinkite (e.g., [8–10]). Minor Fe mineralization, consisting of almost pure hematite-magnetite, was found in the periphery of the Mn ores, close to the wall rock at Kesebol. The Cu ore, known since 1718 [11] consists of mainly chalcocite and chalcopyrite, and is restricted to a few sulfide-rich zones in the deposit [2].

There are different views on the formation of this kind of Mn occurrences in the region. Geijer [2] advocated a primarily epigenetic origin, whereas Boström et al. [12] suggested a genetic relationship to the synsedimentary exhalative Långban-type Mn-Fe-(Ba-Pb-As) deposits in Värmland, ca. 140 km NE of Kesebol (in the ~1.9 Ga Bergslagen ore region).

We consider kesebolite-(Ce) very rare at the deposit; all known samples are from the same piece of rock. It was spotted and collected by one of us (A.P.) in 1991 from a mine dump. It occurs with rhodonite, baryte, quartz, calcite, talc, andradite, rhodochrosite, K-feldspar, hematite, gasparite-(Ce), chernovite-(Y), ferriakasakaite-(Ce) and a possible Mn-analogue to cerite-(Ce). To some extent, kesebolite-(Ce) has also been altered, forming a very fine-grained, porcelain-like light brown-beige aggregate of gasparite-(Ce), calcite, a talc-like mineral and an unknown solid phase, mainly consisting of O, Si, As, Ce and Y as seen from EDS spectra and with low analytical totals.

3. Physical Properties

Kesebolite-(Ce) occurs mostly as euhedral crystals up to 3 mm in the type specimen, in close contact with manganoan calcite, rhodonite, gasparite-(Ce), ferriakasakaite-(Ce) and the possible Mn-analogue of cerite-(Ce) (Figures 1 and 2), in a brecciated, fine-grained andradite skarn. The crystals are short-prismatic along *c*, with lengthwise striation. The major forms are {001}, {100} and {110}. The color of kesebolite-(Ce) is dark brown to grayish brown, with a vitreous luster and a light brown streak. No fluorescence effects were detected in UV light.

Figure 1. The kesebolite-(Ce) (Kbl) type specimen with calcite (white) and rhodonite (reddish), GEO-NRM No. 20100343. Field of view is ca. 5 × 3 mm. Photo: Torbjörn Lorin.
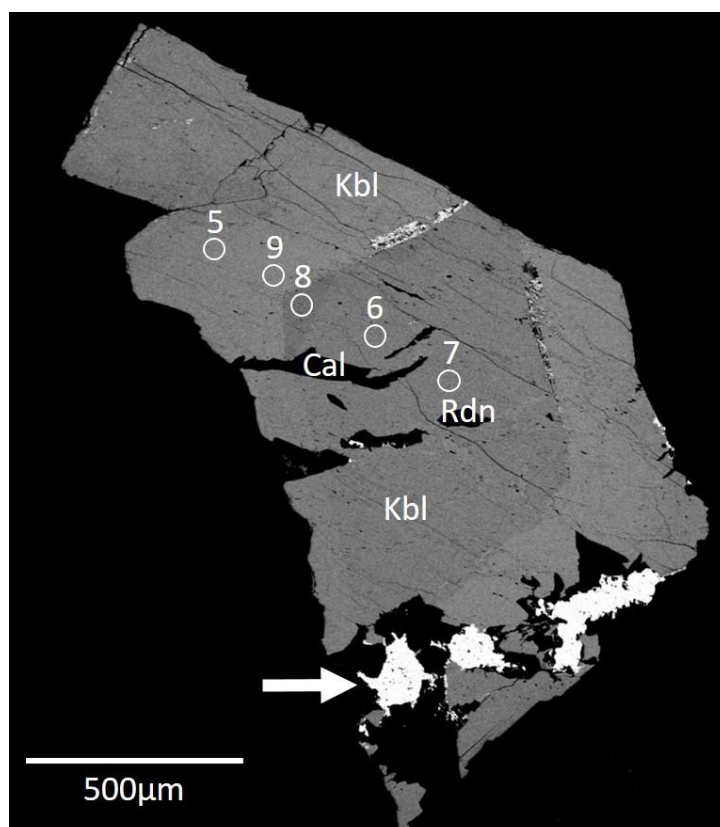

Figure 2. SEM-BSE image (maximum contrast) of a polished section of a kesebolite-(Ce) crystal (Kbl). Patches of rhodonite (Rdn) and manganoan calcite (Cal) occur as inclusions in kesebolite-(Ce); the white arrow points to an intergrowth between gasparite-(Ce) and a possible Mn-analogue to cerite-(Ce). Numbered rings refer to areas of selected point analyses (Tables 2 and 3).

The Mohs hardness is estimated to be 5–6 from scratch tests. From micro-indentation (VHN$_{100}$) measurements using a Shimadzu type-M tester we obtained a mean of 825 (the complete range for 11 indentations is 711–974). The mineral is brittle with irregular fractures; a fair cleavage is observed on {100}. The density was not measured, because of safety regulations concerning heaviest liquids;

the calculated value is 3.998(5) g·cm^{-3} using the empirical formula and unit-cell volume from powder X-ray diffraction data (see below).

Optically, kesebolite-(Ce) is biaxial positive. Pleochroism is weak, in brownish-yellow shades. Refractive indices were not determined directly; the calculated value is 1.740 from Gladstone–Dale constants [13]. Polarized reflectance spectra were measured in air with an AVASPEC-ULS2048×16 spectrometer (Avantes BV, Apeldoorn, The Netherlands) attached to a Zeiss Axiotron UV-microscope (Zeiss, Oberkochen, Germany) (10×/0.20 ultrafluar objective), using a halogen lamp (100 W) and a SiC (Zeiss no. 846) standard, with a circular sample measurement field of 120 μm in diameter. The results from the 400–700 nm range (average of 600 scans, 100 ms integration time) are given in Table 1. Calculated *n* values from the reflectance data using Fresnel's equation are $n_2 = 1.76(2)$, $n_1 = 1.74(2)$ at 589 nm.

Table 1. Reflectance values (%) measured in air (COM wavelengths in italics).

λ (nm)	R_2	R_1	λ (nm)	R_2	R_1
400	8.31	8.10	560	7.65	7.45
420	8.07	7.86	580	7.57	7.38
440	8.03	7.81	*589*	*7.56*	*7.37*
460	7.85	7.62	600	7.55	7.36
470	*7.82*	*7.61*	620	7.59	7.39
480	7.79	7.60	640	7.54	7.38
500	7.71	7.50	*650*	*7.56*	*7.38*
520	7.65	7.46	660	7.58	7.38
540	7.68	7.48	680	7.61	7.42
546	*7.68*	*7.47*	700	7.54	7.35

4. Mineral Chemistry

The chemical composition of kesebolite-(Ce), with respect to the major oxides (SiO_2, SO_3, CaO, MnO and As_2O_5), was determined using an FEI Quanta 650 field-emission scanning electron microscope (hosted by the Swedish Museum of Natural History), fitted with an 80 mm^2 X-MaxN Oxford Instruments EDS detector (Oxford Instruments, High Wycombe, UK) (20 kV, beam size 1 μm, working distance 10 mm). Beam current was calibrated on Co metal, with the instrument calibrated against metal and mineral standards for each element. Three separate crystal fragments were analyzed and the total number of point analyses was 9 (Table 2). A slight chemical zonation indicated by BSE images (Figure 2) is obviously related to variations in Ca and REE (darker and lighter areas, respectively).

All other elements reported including the REE were measured with LA-ICP-MS/MS by an Agilent 8800 instrument coupled to a ESI NWR 213 nm Nd:YAG laser (at the Department of Earth Sciences, University of Gothenburg). Laser spots were set to 30 μm in diameter (close to the points analyzed by EDS) with a laser fluence of ca. 4.9 J/cm^2 at a repetition frequency of 10 Hz. Standardization was achieved by repeatedly analyzing NIST SRM 610 glass as a primary standard, normalizing by taking SiO_2 concentration values based on EDS from the closest analyzed spot. Quantification of the REE in kesebolite-(Ce) with this approach was monitored by analyzing natural xenotime-(Y) and monazite-(Ce) with well-established concentrations. Trace element concentrations are reported in Table 3.

The remaining elements of the periodic table (from Li to U, with the exception of PGE and halogens), not reported in Tables 2 or 3, were analyzed in two points with a 50 μm laser spot diameter in order to evaluate their presence, but they all were found below the detection limit with the current settings. No H_2O or CO_2 contents are indicated by the structural and spectroscopic data, see below.

The empirical formula calculated from the average analysis (Table 2), on the basis of 13 O, is: $(Ce_{0.70}La_{0.12}Nd_{0.09}Pr_{0.03}Sm_{0.01}Y_{0.01})_{\Sigma0.96}(Ca_{2.01}Sr_{0.01})_{\Sigma2.02}(Mn^{2+}_{1.01}Mg_{0.05}Fe^{2+}_{0.01})_{\Sigma1.07}(Si_{3.05}As^{5+}_{0.81}$ $P_{0.06}S^{6+}_{0.04}V^{5+}_{0.02})_{\Sigma3.98}O_{13}$. A simplified formula for kesebolite-(Ce) can be written $(Ce,La,Nd)Ca_2(Mn,Mg)$ $(As,P,Si,S)Si_3O_{13}$. The ideal formula, $CeCa_2Mn(AsO_4)[SiO_3]_3$, requires SiO_2 28.06, As_2O_5 17.89, Ce_2O_3 25.55, CaO 17.46, MnO 11.04, total 100 wt.%.

Table 2. Chemical data (in wt.%) for kesebolite-(Ce).

Method	Oxide	1	2	3	4	5	6	7	8	9	Mean	1σ
ICP-MS	MgO	0.423	0.340	0.215	0.418	0.194	0.189	0.180	0.904	0.145	0.334	0.238
EDS	SiO_2	28.85	29.20	29.14	29.15	28.88	29.24	29.09	29.20	29.10	29.10	0.14
ICP-MS	P_2O_5	0.803	0.961	0.680	0.769	0.488	0.535	0.480	0.463	0.572	0.639	0.175
EDS	SO_3	0.28	0.52	0.24	0.55	0.36	0.70	0.62	1.25	0.31	0.54	0.31
EDS	CaO	17.70	18.00	17.44	17.96	17.64	18.07	18.08	18.86	17.36	17.90	0.45
ICP-MS	V_2O_5	0.342	0.370	0.401	0.364	0.410	0.181	0.181	0.208	0.407	0.318	0.099
EDS	MnO	11.44	11.47	11.14	11.36	11.44	11.35	11.37	11.72	11.31	11.40	0.16
ICP-MS	FeO	0.140	0.159	0.136	0.160	0.133	0.277	0.266	0.144	0.069	0.165	0.066
ICP-MS	ZnO	0.012	0.011	0.012	0.011	0.011	0.012	0.011	0.014	0.009	0.012	0.001
EDS	As_2O_5	14.78	14.53	14.82	14.38	14.89	14.53	14.65	15.13	15.00	14.74	0.24
ICP-MS	SrO	0.100	0.094	0.106	0.095	0.106	0.105	0.105	0.109	0.109	0.103	0.006
ICP-MS	Y_2O_3	0.259	0.263	0.241	0.278	0.320	0.169	0.162	0.174	0.327	0.243	0.063
ICP-MS	La_2O_3	3.163	3.514	3.377	3.048	2.867	2.015	2.090	2.293	2.863	2.803	0.550
ICP-MS	Ce_2O_3	18.572	18.254	19.035	18.355	18.534	17.541	17.982	16.593	18.679	18.171	0.730
ICP-MS	Pr_2O_3	0.687	0.578	0.647	0.582	0.763	0.846	0.869	0.755	0.718	0.716	0.104
ICP-MS	Nd_2O_3	2.386	1.942	2.243	2.062	2.844	3.704	3.832	3.040	2.750	2.756	0.679
ICP-MS	Sm_2O_3	0.201	0.183	0.183	0.209	0.236	0.323	0.322	0.251	0.248	0.240	0.053
ICP-MS	PbO	0.125	0.101	0.129	0.103	0.126	0.106	0.110	0.122	0.126	0.116	0.011
ICP-MS	Bi_2O_3	0.016	0.015	0.016	0.016	0.018	0.020	0.020	0.025	0.020	0.019	0.003
ICP-MS	ThO_2	0.109	0.033	0.138	0.024	0.055	0.041	0.051	0.040	0.060	0.061	0.038
	Total	100.39	100.53	100.34	99.89	100.32	99.96	100.48	101.30	100.18	100.38	

Table 3. LA-ICP-MS trace element data (in μg/g) for kesebolite-(Ce).

Element	1	2	3	4	5	6	7	8	9	Mean
Al	3.9	3.3	2.5	8.6	243.8	6.9	7.8	15.2	4.7	33.0
Sc	4.3	3.1	4.3	3.5	3.3	4.4	4.3	2.9	3.4	3.7
Zr	15.2	11.6	21.1	10.1	18.2	13.7	13.6	8.6	17.4	14.4
Ba	18.1	30.1	19.8	13.6	4.1	8.2	1.7	12.3	7.7	12.9
Eu	241.9	245.0	223.6	282.2	277.0	323.6	326.5	259.9	296.5	275.1
Gd	847.7	903.9	801.8	1064.9	963.4	886.7	899.5	737.4	1001.3	900.7
Tb	62.5	68.9	58.7	77.6	72.8	53.1	52.3	46.2	74.5	62.9
Dy	258.4	281.9	249.0	303.8	310.3	194.5	191.1	183.0	316.7	254.3
Ho	38.4	40.3	37.3	42.7	47.4	26.3	26.0	26.4	47.4	36.9
Er	77.0	76.7	73.4	78.5	96.4	50.1	48.3	53.6	97.0	72.3
Tm	7.1	6.8	6.8	6.9	9.1	4.7	4.8	5.1	9.1	6.7
Yb	35.1	30.8	34.0	31.9	45.5	24.1	24.6	26.1	46.4	33.2
Lu	4.9	4.4	4.9	4.5	5.9	3.2	3.2	3.9	6.1	4.6

5. X-ray Crystallography

Powder X-ray diffraction data (Figure 3 and Table 4) were collected with a PANalytical X'Pert³ powder diffractometer equipped with an X'celerator silicon-strip detector and operated at 40 mA and 45 kV (CuKα-radiation, λ = 1.5406 Å). Bragg peak positions were determined with the PANalytical HighScorePlus 4.6 software (Malvern Panalytical, Kassel, Germany) and corrected against an external Si standard (NBS 640b). Monoclinic unit-cell parameters refined from the powder data are *a* = 6.7408(8) Å, *b* = 13.0133(15), *c* = 12.0649(20) Å, β = 98.504(13)° and *V* = 1046.67(17) Å³.

Single-crystal X-ray diffraction measurements were carried out at CRIST (Centro di Cristallografia of the University of Florence) on a crystal fragment (size 30 × 40 × 70 μm) of kesebolite-(Ce) using a Bruker D8 Venture equipped with a Photon II CCD detector, with graphite-monochromatized MoKα radiation (λ = 0.71073 Å), working at 60 kV with 15 s exposure time per frame; the detector-to-sample distance was 6 cm. The intensity data were integrated and corrected for standard Lorentz polarization factors with the software package APEX3 [14]. A total of 4636 unique reflections was collected up to 2θ = 70.08°. The reflection conditions (*h0l*: *h* = 2*n*; *0k0*: *k* = 2*n*; *00l*: *l* = 2*n*) pointed unequivocally to the space group $P2_1/c$, and thus the structure solution was undertaken in this space group. The positions of the majority of the atoms (three *A* sites = Ca and REE; *M* = Mn and *T*1 = Si, As cations) were determined by means of direct methods [15]. A least squares refinement on F^2 using these heavy-atom positions

and isotropic temperature factors produced an *R* factor of 0.156. Three-dimensional difference Fourier synthesis yielded the position of the remaining *T* cations (Si) and thirteen O atoms.

Table 4. X-ray powder diffraction data (*d* in Å) for kesebolite-(Ce).

I	d_{obs}	d_{calc}	h	k	l	I_{calc}
8	6.66	6.666	1	0	0	3
11	6.50	6.507	0	2	0	3
29	5.96	5.966	0	0	2	42
24	5.70	5.713	0	2	1	28
8	5.43	5.423	0	1	2	3
5	5.05	5.054	1	1	1	8
6	4.81	4.814	1	0	−2	5
5	4.66	4.656	1	2	0	6
18	4.50	4.498	−1	2	1	22
6	4.40	4.397	0	2	2	4
9	4.19	4.194	1	2	1	9
25	3.512	3.508	0	3	2	23
9	3.393	3.3936	0	2	3	9
57	3.228	3.2290	2	1	0	48
84	3.138	3.1388	0	4	1	45
100	3.114	3.1125	2	0	−2	100
40	3.024	3.0271	−2	1	2	6
48	3.002	2.9991	1	3	2	25
92	2.924	2.9238	1	4	0	9
72	2.908	2.9076	0	1	4	37
40	2.883	2.8833	−1	4	1	25
48	2.856	2.8563	0	4	2	44
37	2.793	2.7941	2	2	1	27
25	2.740	2.7423	2	0	2	19
41	2.696	2.6954	−1	4	2	22
43	2.684	2.6834	2	1	2	27
22	2.581	2.5819	1	3	3	16
18	2.529	2.5288	−2	3	2	9
18	2.427	2.4245	1	5	0	8
17	2.331	2.3308	−2	4	1	9
9	2.284	2.2861	1	4	3	6
18	2.241	2.2420	2	4	1	8
16	2.214	2.2125	−3	1	1	11
40	2.123	2.1224	−3	2	1	20
36	2.106	2.1064	−2	4	3	18
19	2.077	2.0765	−3	2	2	5
24	2.050	2.0496	2	1	4	8
18	2.025	2.0235	1	4	4	5
19	1.995	1.9966	−2	5	2	8
15	1.978	1.9777	3	3	0	6
20	1.925	1.9243	0	4	5	8
17	1.836	1.8369	0	7	1	5
40	1.818	1.8179	2	6	0	6
27	1.677	1.6762	2	3	5	20

The program SHELXL [15] was used for the refinement of the structure. The occupancy of all the sites was left free to vary (Ca vs. Ce at the *A* sites; Mn vs. structural vacancy at the Mn site; Si vs. As at the *T* sites) and then fixed to the resulting value. Neutral scattering curves were taken from the International Tables for X-ray Crystallography [16]. At the last stage, with an-isotropic atomic displacement parameters for all atoms and no constraints, the residual value settled at *R* = 0.0456 for 3282 observed reflections (2σ(*I*) level) and 195 parameters and at *R* = 0.0780 for all 4636 independent reflections. A crystallographic information file with the full experimental data is available (see Supplementary Material). Experimental details and *R* indices are given in Table 5. Fractional atomic coordinates and isotropic displacement parameters are reported in Table 6. Bond distances are given in Table 7, and the corresponding bond-valence calculation [17] is presented in Table 8.
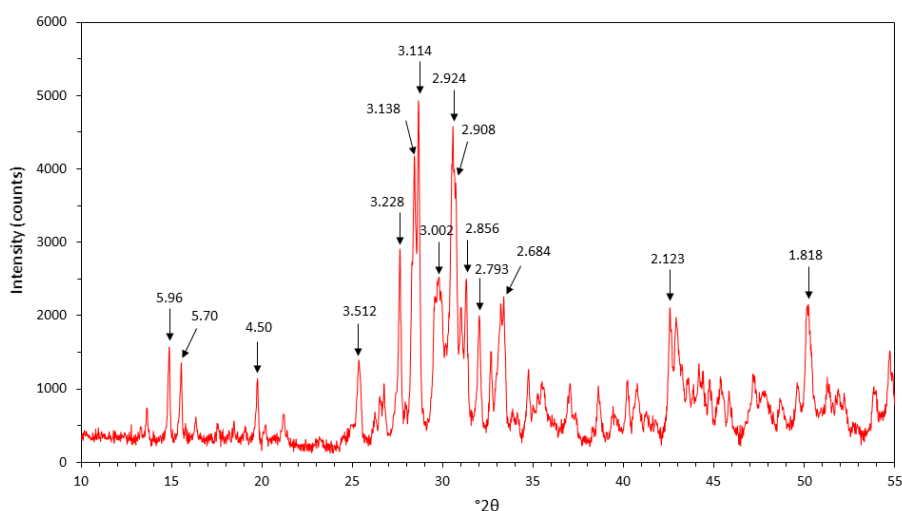
Figure 3. Powder X-ray diffractogram of kesebolite-(Ce). Major Bragg peaks are labeled with the corresponding *d* values (in Å).

Table 5. Crystal data and experimental conditions for the single-crystal XRD study.

Crystal Data	
Ideal formula	$CeCa_2Mn(AsO_4)[SiO_3]_3$
Crystal size (mm^3)	$0.030 \times 0.040 \times 0.070$
Form	Block
Color	Brown
Crystal system	monoclinic
Space group	$P2_1/c$
a (Å)	6.7382(3)
b (Å)	13.0368(6)
c (Å)	12.0958(6)
β (°)	98.578(2)
V (Å^3)	1050.66(9)
Z	4
Data Collection	
Instrument	Bruker D8 Venture
Radiation type	$MoK\alpha$ (λ = 0.71073 Å)
Temperature (K)	293(3)
Detector to sample distance (cm)	6
Number of frames	558
Measuring time (s)	15
Maximum covered 2θ (°)	70.08
Absorption correction	multi-scan
Collected reflections	29,156
Unique reflections	4636
Reflections with $F_o > 4\sigma(F_o)$	3282
R_{int}	0.0518
R_σ	0.0679
Range of h, k, l	$-10 \leq h \leq 10, -20 \leq k \leq 21, -19 \leq l \leq 17$
Refinement	
Refinement	Full-matrix least squares on F^2
Final R_1 ($F_o > 4\sigma(F_o)$)	0.0456
Final R_1 (all data)	0.0780
S	1.056
Number refined parameters	195
$\Delta\rho_{max}$ (e Å^{-3})	1.65
$\Delta\rho_{min}$ (e Å^{-3})	-1.80

Table 6. Atoms, site-occupancy factors (s.o.f.) and fractional atomic coordinates of kesebolite-(Ce).

Atom	s.o.f.	x	y	z	U_{iso}
A1	$Ca_{0.820(3)}Ce_{0.180}$	0.83660(11)	0.62536(6)	0.46244(6)	0.0254(2)
A2	$Ca_{0.947(3)}Ce_{0.053}$	0.72998(16)	0.92143(10)	0.45402(9)	0.0351(4)
A3	$Ce_{0.722(4)}Ca_{0.278}$	0.46715(5)	0.66905(3)	0.21399(3)	0.02051(12)
M	$Mn_{1.000}$	0.93729(12)	0.50166(7)	0.73249(7)	0.0237(2)
T1	$As_{0.715(5)}Si_{0.285}$	0.91583(9)	0.75860(5)	0.69620(5)	0.0216(2)
T2	$Si_{1.000}$	0.3178(2)	0.63806(11)	0.48162(11)	0.0177(3)
T3	$Si_{1.000}$	0.4110(2)	0.56509(11)	0.72491(11)	0.0180(3)
T4	$Si_{1.000}$	0.2390(2)	0.86114(11)	0.42920(11)	0.0187(3)
O1	$O_{1.000}$	0.4138(6)	0.6384(3)	0.6156(3)	0.0241(7)
O2	$O_{1.000}$	0.2522(5)	0.4732(3)	0.7102(3)	0.0222(7)
O3	$O_{1.000}$	0.6294(6)	0.5175(3)	0.7700(3)	0.0247(7)
O4	$O_{1.000}$	0.3640(6)	0.6501(3)	0.8204(3)	0.0243(7)
O5	$O_{1.000}$	0.4972(6)	0.6434(3)	0.4109(3)	0.0235(7)
O6	$O_{1.000}$	0.1627(6)	0.5456(3)	0.4505(3)	0.0245(7)
O7	$O_{1.000}$	0.0487(6)	0.9346(3)	0.4012(3)	0.0281(8)
O8	$O_{1.000}$	0.3956(6)	0.9094(3)	0.5286(3)	0.0294(8)
O9	$O_{1.000}$	0.1827(6)	0.7448(3)	0.4644(3)	0.0242(7)
O10	$O_{1.000}$	0.7877(6)	0.7533(3)	0.8042(3)	0.0278(8)
O11	$O_{1.000}$	0.1092(6)	0.8394(3)	0.7202(4)	0.0272(8)
O12	$O_{1.000}$	0.7511(7)	0.8023(4)	0.5907(4)	0.0392(11)
O13	$O_{1.000}$	0.9755(7)	0.6459(3)	0.6545(4)	0.0308(9)

Table 7. Selected interatomic distances (Å) for kesebolite-(Ce).

Distance	Value	Distance	Value
A1—O5	2.291(4)	M—O13	2.136(5)
A1—O13	2.387(4)	M—O3	2.198(4)
A1—O2	2.449(4)	M—O2	2.210(4)
A1—O6	2.455(4)	M—O11	2.226(4)
A1—O6	2.464(4)	M—O7	2.228(4)
A1—O10	2.466(4)	M—O6	2.300(4)
A1—O9	2.802(4)	<M—O>	2.216
A1—O12	2.886(6)		
<A1—O>	2.525	T1—O13	1.623(4)
		T1—O12	1.662(4)
A2—O12	2.258(5)	T1—O10	1.671(4)
A2—O7	2.337(4)	T1—O11	1.667(4)
A2—O3	2.366(4)	<T1—O>	1.656
A2—O8	2.382(5)		
A2—O8	2.554(4)	T2—O5	1.583(4)
A2—O7	2.834(5)	T2—O6	1.603(4)
A2—O4	2.894(4)	T2—O1	1.653(4)
A2—O10	2.972(4)	T2—O9	1.659(4)
<A2—O>	2.575	<T2—O>	1.642
A3—O5	2.384(4)	T3—O2	1.598(4)
A3—O11	2.427(4)	T3—O3	1.615(4)
A3—O8	2.446(4)	T3—O1	1.634(4)
A3—O1	2.486(4)	T3—O4	1.665(4)
A3—O3	2.533(4)	<T3—O>	1.638
A3—O12	2.622(5)		
A3—O2	2.709(4)	T4—O7	1.596(4)
A3—O1	2.778(4)	T4—O8	1.606(4)
A3—O4	2.823(4)	T4—O9	1.635(4)
<A3—O>	2.579	T4—O4	1.671(4)
		<T4—O>	1.636

Table 8. Calculated bond-valence sums (BVS, in valence unit, i.e., v.u.).

	*A*1	*A*2	*A*3	*M*	*T*1	*T*2	*T*3	*T*4	ΣO
	$Ca_{0.82}Ce_{0.18}$	$Ca_{0.95}Ce_{0.05}$	$Ce_{0.72}Ca_{0.28}$	$Mn_{1.00}$	$As_{0.72}Si_{0.28}$	$Si_{1.00}$	$Si_{1.00}$	$Si_{1.00}$	
O1			0.147			0.925	0.985		2.057
O2	0.305		0.201	0.321			1.120		1.947
O3		0.352	0.323	0.332			1.070		2.077
O4		0.085	0.147				0.935	0.920	2.087
O5	0.468		0.483			1.167			2.118
O6	0.300, 0.293			0.252		1.105			1.950
O7		0.381, 0.099		0.306				1.126	1.912
O8		0.337, 0.212	0.409					1.096	2.054
O9	0.118					0.950		1.014	2.082
O10	0.292	0.068	0.366		1.192				1.918
O11		0.430		0.308	1.199				1.937
O12	0.093	0.471	0.254		1.218				2.036
O13	0.360			0.393	1.354				2.107
	2.229	2.004	2.779	1.912	4.962	4.147	4.110	4.156	

In the crystal structure of kesebolite-(Ce), markedly wavy, 6-periodic single tetrahedral (*T*2 + *T*3 + *T*4) chains run along (001) and are interconnected by corner sharing to infinite (010) strings formed by alternating, corner-sharing *M*-octahedra and *T*1-tetrahedra. In a projection along the (100) axis, the structure appears as a trellis-like framework (Figure 4a), with *A*1, *A*2 and *A*3 sites occupying the remaining voids (Figure 4b).
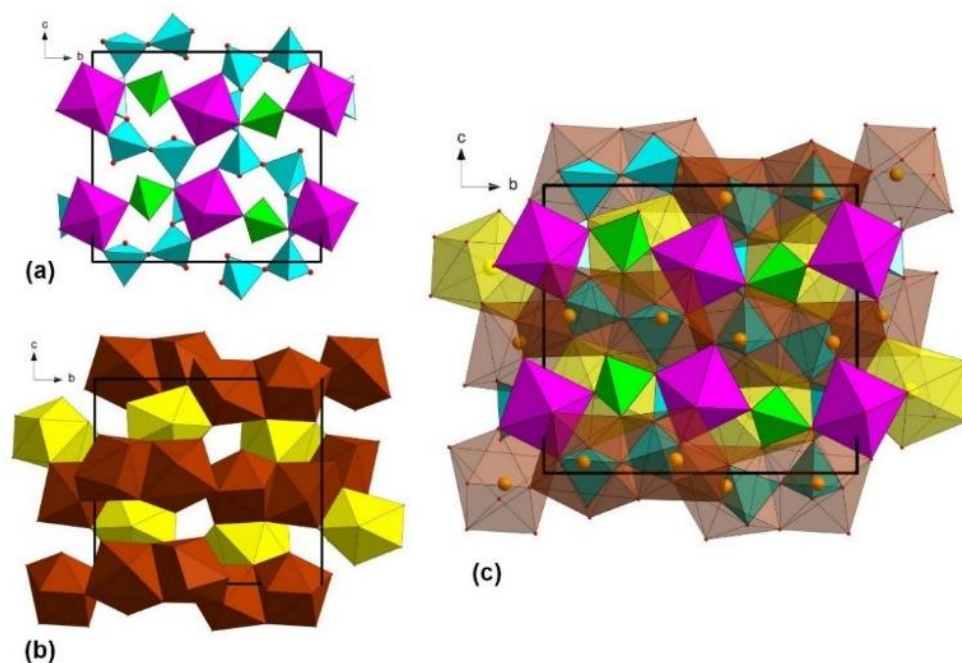

Figure 4. The crystal structure of kesebolite-(Ce) viewed along the a axis. Square corresponds to the unit-cell edges. (**a**) Si-tetrahedra are colored in turquoise; As-tetrahedra and Mn-octahedra in green and pink, respectively. (**b**) *A*1 and *A*2 polyhedra (Ca) in red, *A*3 (Ce) in yellow. (**c**) The total structure with all polyhedra shown (partly transparent). Ca atoms as orange spheres, Ce in yellow.

The *T*2, *T*3 and *T*4 sites are occupied by Si alone, with <Si–O> distances varying between 1.636 and 1.642 Å. As^{5+} is completely ordered at *T*1, which shows a mean distance of 1.656 Å, longer than the other tetrahedral distances. Indeed, the crystal-structure refinement of *T*1 occupancy points to a site scattering of 27.6 electrons, corresponding to a site population ($As_{0.715}Si_{0.285}$). Taking into account the ionic radii established by [18] for four-fold coordinated As^{5+} and Si^{4+} (0.335 and 0.26 Å, respectively)

and three-fold coordinated O^{2-} (1.36 Å), the expected <$T1$–O> value (1.674 Å) is reasonably in accord with the experimental data.

Mn^{2+} at the *M* site shows a slightly distorted octahedral coordination, with an average bond distance of 2.216 Å. Such a value is in keeping with those observed in arsenmedaite, $Mn^{2+}_6As^{5+}Si_5O_{18}OH$ (range 2.196–2.218 Å; [19]) and with the ideal <Mn–O> distance (2.19 Å) calculated using the ionic radii of $^{VI}Mn^{2+}$ and $^{III}O^{2-}$ [17]. Actually, oxygen atoms are three- and four-fold coordinated here, and consequently the ideal calculated average <Mn–O> distance should be slightly larger (~2.20 Å). The *A*1 and *A*2 sites, dominated by Ca, are eight-fold coordinated (average bond distance = 2.525 and 2.575 Å, respectively), whereas *A*3, which hosts REE cations, is nine-fold coordinated (average bond distance = 2.579 Å).

The bond valence sums (BVS in Table 8) at the *T* sites of kesebolite-(Ce) range between 4.11 and 4.16 v.u. for the Si-centered tetrahedra and it is 4.96 v.u. for *T*1, which is mainly occupied by As^{5+}. The BVSs of the oxygen atoms range between 1.91 and 2.12 v.u., which rules out the presence of OH^- groups in the structure.

Kesebolite-(Ce) fits in the Strunz group 9.DM (inosilicates with 6-periodic single chains).

6. Micro-Raman Spectroscopy

Raman-spectroscopy measurements were carried out at room temperature using a Horiba (Jobin Yvon) LabRam HR Evolution, at the Department of Earth Sciences, University of Gothenburg. The samples were excited with an air-cooled, frequency doubled 532 nm Nd-YAG laser utilizing an Olympus 100× objective (numerical aperture = 0.9). Spectra were generated in the range of 25 to 4000 cm^{-1} utilizing a 600 grooves/cm grating. The spectral resolution on randomly oriented polished crystals of kesebolite-(Ce) was in the order of 1 cm^{-1}. The lateral resolution was in the order of 1 μm. The wavenumber calibration was done using the 520.7 cm^{-1} Raman band on a polished silicon wafer; it showed a wavenumber accuracy usually better than 0.5 cm^{-1}. Raman spectra of the sample were collected through 10 acquisition cycles with single counting times of 30 s in a close to back-scattered geometry. Separate spectra were collected in two distinct zones (visible in BSE, see Figure 2) of the crystals, both of which yield similar Raman spectra (Figure 5).
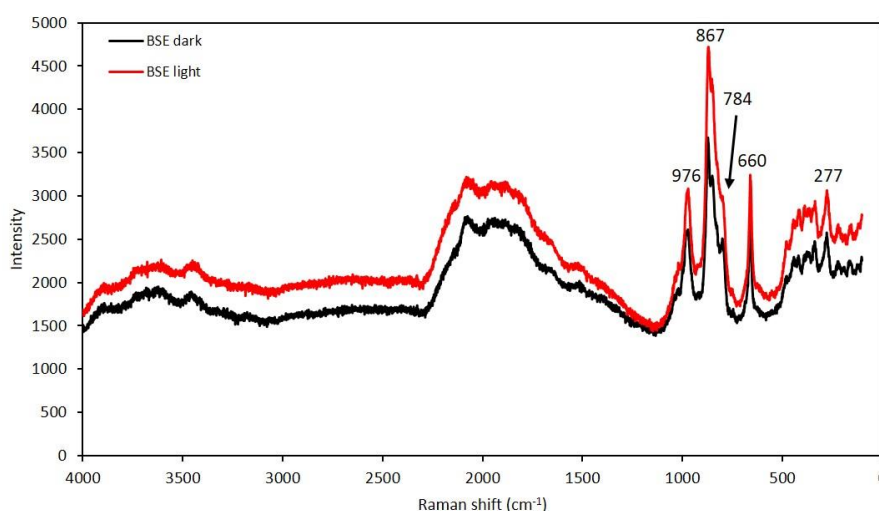

Figure 5. Raman spectra of kesebolite-(Ce) from different areas of the grain shown in Figure 2.

The strongest band at 867 cm^{-1} could tentatively be assigned to antisymmetric stretching of the AsO_4^{3-} groups and the slightly weaker band at 784 cm^{-1} to symmetric stretching mode of the same groups [20]. The strong band at 976 cm^{-1} is likely related to the asymmetric vibration mode of the $[SiO_3]$-groups and the one at 660 cm^{-1} to bending mode of the same functional group [21]. The weaker bands at lower wavenumbers (300 to 450 cm^{-1}) could be attributed to bending and stretching modes

of Mn-O and out of plane bending modes of the AsO_4^{3-} group [22]. The very broad spectral features from 1300 cm^{-1} are probably fluorescence effects.

7. Discussion

The chemical composition obtained from structure refinement (Table 6) of kesebolite-(Ce), $Ce_{0.96}Ca_{2.04}Mn_{1.00}(As_{0.72}Si_{0.28})Si_3O_{13}$, is in reasonably good agreement with the above empirical formula. The calculated bond valences (Table 8) confirm the overall structural model. As discussed above, the average $T1$-O bond distance of 1.656 Å is rather short when compared to what is expected from a pure, tetrahedrally coordinated As^{5+}-site (around 1.69 Å; [23]), but explained by the incorporation of smaller ions (Si^{4+} and minor amounts of P^{5+} and S^{6+}) replacing As^{5+}. The crystal-chemical role of hexavalent S should be noted. There is a clear antipathetic variation of S vs. REE in kesebolite-(Ce) and sympathetic S vs. Ca (Figure 6), indicating the occurrence of the heterovalent substitution mechanism $REE^{3+} + As^{5+} \rightarrow Ca^{2+} + S^{6+}$. The zonation pattern seen in the BSE images of kesebolite-(Ce) (Figure 2) is mainly related to this coupled variation. SO_4^{2-}-for-AsO_4^{3-} replacement is not very common in minerals but has been documented, e.g., members of the tsumcorite group [24] and for synthetic jarosite [25] and ettringite [26].
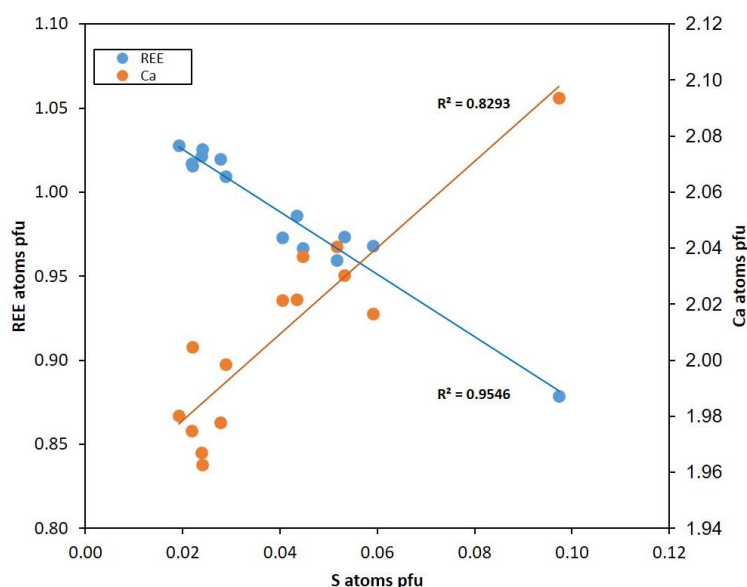

Figure 6. Compositional variations in kesebolite-(Ce). The straight lines are obtained from linear fits of the data.

The crystal structure of kesebolite-(Ce) is of a novel type, with a unique topology, and it is the only known mineral with essential Ce, Ca, Mn, As and Si. It has the same metal:As:Si:O ratio as tiragalloite, $Mn_4[AsSi_3O_{12}(OH)]$, but exhibits a different structural topology. In tiragalloite and related arsenmedaite, As-tetrahedra are part of terminated silicate chains [18,27]. Braccoite, $NaMn^{2+}_5[Si_5AsO_{17}(OH)](OH)$, has pyroxenoid-like infinite silicate chains with the As-tetrahedra included [28].

Kesebolite-(Ce) is rather unique among Mn-As silicate minerals in that it is not protonated. In contrast to the above mentioned related minerals, belonging to late-stage vein systems developed at zeolite to prehnite-pumpellyite facies conditions, kesebolite-(Ce) likely formed at higher temperatures without a significant contribution from mobilization of hydrothermal fluids. Overall, the present paragenesis constitutes a "dry" skarn assemblage.

The chondrite-normalized REE pattern of kesebolite-(Ce) indicates significant Ce-enrichment (Figure 7) in the deposit. The other REE minerals from the same deposit exhibit the same pattern. The positive Ce-anomaly is typical of hydrogenetic Mn deposits whereas hydrothermal-sedimentary Mn

ores normally have negative (or no) Ce anomalies [29,30]. Under those conditions, a Ce-enriched REE source formed from oxidation of Ce^{3+} to Ce^{4+} (with the formation of insoluble CeO_2). The precursors to the Mn ore at Kesebol likely precipitated in an oxic, possibly marine environment, like the Långban-type deposits [12,31]. At present it cannot, however, be concluded if co-precipitation of REE and Mn (plus As) actually occurred, or if REE is derived from a detrital source. Subsequent reworking and neo-mineralization in one or more phases of the Sveconorwegian orogeny could lead to the so far unique, essentially anhydrous Mn-As-REE mineral assemblage.
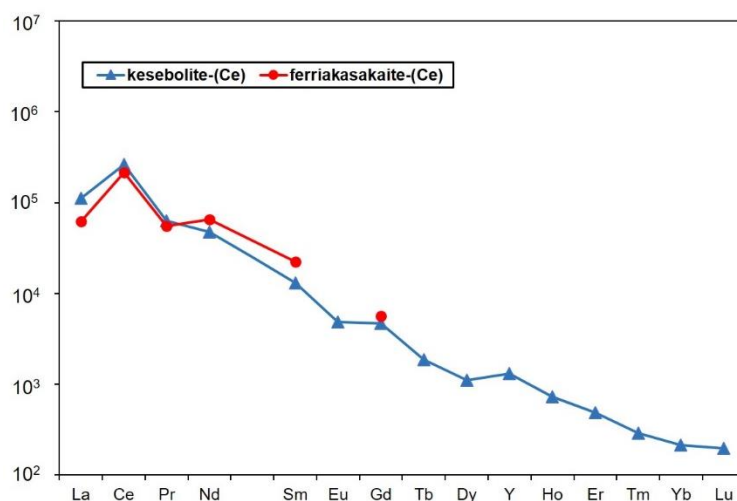
Figure 7. Chondrite-normalized REE pattern for kesebolite-(Ce) compared with ferriakasakaite-(Ce) based on ICP-MS analyses. Chemical data for ferriakasakaite-(Ce) from Kesebol (EPMA-WDS data) are taken from [10].

References

1. Sølver, S.V. *Undersökning av en Stuffsamling från Kesebol i Dalsland Report*; Royal Institute of Technology: Stockholm, Sweden, 1942; 28p.

2. Geijer, P. The manganese, iron and copper mineralization at Kesebol in Dalsland, southwestern Sweden. *Bull. Geol. Inst. Upps. New Ser.* **1961**, *40*, 37–49.

3. Lindström, S. *Längs Tösse-Tydjeån. Människorna, Industrierna, Gruvan i Kesebol*; AB Åmålstryck: Åmål, Sweden, 1988; 170p.

4. Åhäll, K.-I.; Connelly, J.N. Long-term convergence along SW Fennoscandia: 330 m.y. of Proterozoic crustal growth. *Precambrian Res.* **2008**, *161*, 452–474. [CrossRef]

5. Andreasson, P.-G.; Solyom, Z.; Johansson, I. Geotectonic significance of Mn-Fe-Ba and Pb-Zn-Cu-Ag mineralizations along the Sveconorwegian-Grenvillian Front in Scandinavia. *Econ. Geol.* **1987**, *82*, 201–207. [CrossRef]

6. Alm, E. Sveconorwegian Metallogenesis in Sweden. Ph.D. Thesis, Stockholm University, Stockholm, Sweden, 2000.

7. Romer, R.L.; Wright, J.E. Lead mobilization during tectonic reactivation of the western Baltic Shield. *Geochim. Cosmochim. Acta* **1993**, *57*, 2555–2570. [CrossRef]

8. Kolitsch, U.; Holtstam, D.; Gatedal, K. Crystal chemistry of REEXO$_4$ compounds (X = P, As, V) I. Paragenesis and crystal structure of phosphatian gasparite-(Ce) from the Kesebol Mn-Fe-Cu deposit, Västra Götaland, Sweden. *Eur. J. Miner.* **2004**, *16*, 111–116. [CrossRef]

9. Nysten, P.; Holtstam, D. Crystal chemical data on Mn-rich "allanite" from the Harstigen and Kesebol Mn deposits, west-central Sweden. In Proceedings of the CER200—Rare Earth Minerals Mineralogical Society of Sweden, Stockholm, Sweden, September 2004; Volume GFF 127, pp. 33–41.

10. Bonazzi, P.; Holtstam, D.; Bindi, L.; Nysten, P.; Capitani, G. Multi-analytical approach to solve the puzzle of an allanite-subgroup mineral from Kesebol, Västra Götaland, Sweden. *Am. Miner.* **2009**, *94*, 121–134. [CrossRef]

11. Lignell, A. *Beskrifning Öfver Grefskapet Dal, I-II*; Norstedts: Stockholm, Sweden, 1851; 446p.

12. Boström, K.; Rydell, H.; Joensuu, O. Långban; an exhalative sedimentary deposit? *Econ. Geol.* **1979**, *74*, 1002–1011. [CrossRef]

13. Mandarino, J.A. The Gladstone-Dale relationship; Part IV, The compatibility concept and its application. *Can. Miner.* **1981**, *19*, 441–450.

14. *Bruker APEX3, SAINT and SADABS*; Bruker AXS Inc.: Madison, WI, USA, 2016.

15. Sheldrick, G.M. A short history of SHELX. *Acta Crystallogr. Sect. A Found. Crystallogr.* **2008**, *A64*, 112–122. [CrossRef]

16. Wilson, A.J.C. (Ed.) *International Tables for Crystallography, Volume C: Mathematical, Physical and Chemical Tables*; Kluwer Academic: Dordrecht, The Netherlands, 1992.

17. Brese, N.E.; O'Keeffe, M. Bond-valence parameters for solids. *Acta Crystallogr. Sect. B Struct. Sci.* **1991**, *47*, 192–197. [CrossRef]

18. Shannon, R.D. Revised effective ionic radii and systematic studies of interatomic distances in halides and chalcogenides. *Acta Crystallogr. Sect. A Cryst. Phys. Diffr. Theor. Gen. Crystallogr.* **1976**, *32*, 751–767. [CrossRef]

19. Biagioni, C.; Belmonte, D.; Carbone, C.; Cabella, R.; Zaccarini, F.; Balestra, C. Arsenmedaite, $Mn_6^{2+}As^{5+}Si_5O_{18}(OH)$, the arsenic analogue of medaite, from the Molinello mine, Liguria, Italy: Occurrence and crystal structure. *Eur. J. Miner.* **2019**, *31*, 117–126. [CrossRef]

20. Myneni, S.C.; Traina, S.J.; Waychunas, G.A.; Logan, T.J. Experimental and theoretical vibrational spectroscopic evaluation of arsenate coordination in aqueous solutions, solids, and at mineral-water interfaces. *Geochim. Cosmochim. Acta* **1998**, *62*, 3285–3300. [CrossRef]

21. Dowty, E. Vibrational interactions of tetrahedra in silicate glasses and crystals. *Phys. Chem. Miner.* **1987**, *14*, 122–138. [CrossRef]

22. Frost, R.L.; Lopez, A.; Xi, Y.; Scholz, R.; Gandini, A.L. A vibrational spectroscopic study of the silicate mineral ardennite-(As). *Spectrochim. Acta Part A: Mol. Biomol. Spectrosc.* **2014**, *118*, 987–991. [CrossRef]

23. Nagashima, M.; Armbruster, T. Palenzonaite, berzeliite, and manganberzeliite: $(As^{5+}, V^{5+}, Si^{4+})O_4$ tetrahedra in garnet structures. *Miner. Mag.* **2012**, *76*, 1081–1097. [CrossRef]

24. Krause, W.; Belendorff, K.; Bernhardt, H.-J.; McCammon, C.; Effenberger, H.; Mikenda, W. Crystal chemistry of the tsumcorite-group minerals. New data on ferrilotharmeyerite, tsumcorite, thometzekite, mounanaite, helmutwinklerite, and a redefinition of gartrellite. *Eur. J. Miner.* **1998**, *10*, 179–206. [CrossRef]

25. Paktunc, D.; Dutrizac, J.E. Characterization of arsenate-for-sulfate substitution in synthetic jarosite using X-ray diffraction and X-ray absorption spectroscopy. *Can. Miner.* **2003**, *41*, 905–919. [CrossRef]

26. Wang, W.; Shao, Y.; Hou, H.; Zhou, M. Synthesis and thermodynamic properties of arsenate and sulfate-arsenate ettringite structure phases. *PLoS ONE* **2017**, *12*, e0182160. [CrossRef]

27. Nagashima, M.; Armbruster, T. Ardennite, tiragalloite and medaite: Structural control of $(As^{5+}, V^{5+}, Si^{4+})O_4$ tetrahedra in silicates. *Miner. Mag.* **2010**, *74*, 55–71. [CrossRef]

28. Cámara, F.; Bittarello, E.; Ciriotti, M.E.; Nestola, F.; Radica, F.; Marchesini, M. As-bearing new mineral species from Valletta mine, Maira Valley, Piedmont, Italy: II. Braccoite, $NaMn^{2+}_5[Si_5AsO_{17}(OH)](OH)$, description and crystal structure. *Miner. Mag.* **2015**, *79*, 171–189. [CrossRef]

29. Bau, M.; Schmidt, K.; Koschinsky, A.; Hein, J.; Kuhn, T.; Usui, A. Discriminating between different genetic types of marine ferro-manganese crusts and nodules based on rare earth elements and yttrium. *Chem. Geol.* **2014**, *381*, 1–9. [CrossRef]

30. Maynard, J. The Chemistry of Manganese Ores through Time: A Signal of Increasing Diversity of Earth-Surface Environments. *Econ. Geol.* **2010**, *105*, 535–552. [CrossRef]

31. Holtstam, D.; Mansfeld, J. Origin of a carbonate-hosted Fe-Mn-(Ba-As-Pb-Sb-W) deposit of Långban-type in central Sweden. *Miner. Depos.* **2001**, *36*, 641–657. [CrossRef]